



|                  |  |
|------------------|--|
| Title            | Influence of disturbances and environmental changes on albedo in tropical peat ecosystems  |
| Author(s)        | Ohkubo, Shinjiro; Hirano, Takashi; Kusin, Kitso  |
| Citation         | Agricultural and forest meteorology, 301, 108348<br><a href="https://doi.org/10.1016/j.agrformet.2021.108348">https://doi.org/10.1016/j.agrformet.2021.108348</a>  |
| Issue Date       | 2021-05-15   |
| Doc URL          | <a href="http://hdl.handle.net/2115/89225">http://hdl.handle.net/2115/89225</a>  |
| Rights           | © 2021. This manuscript version is made available under the CC-BY-NC-ND 4.0 license<br><a href="http://creativecommons.org/licenses/by-nc-nd/4.0/">http://creativecommons.org/licenses/by-nc-nd/4.0/</a> |
| Rights(URL)      | <a href="http://creativecommons.org/licenses/by-nc-nd/4.0/">http://creativecommons.org/licenses/by-nc-nd/4.0/</a>  |
| Type             | article (author version)   |
| File Information | AlbedoRe3_MS.pdf   |



[Instructions for use](#)

1 **Title:**

2 Influence of disturbances and environmental changes on albedo in tropical peat  
3 ecosystems

4

5 **Authors:**

6 \*Shinjiro Ohkubo<sup>a</sup>, Takashi Hirano<sup>a</sup> and Kitso Kusin<sup>b</sup>

7 \*Corresponding author

8 E-mail: sohkubo@env.agr.hokudai.ac.jp

9

10 <sup>a</sup> Research Faculty of Agriculture, Hokkaido University, Sapporo 060-8589, Japan

11 <sup>b</sup> CIMTROP, University of Palangkaraya, Palangkaraya, 73112, Indonesia

12

13 **Keywords:**

14 Deforestation

15 Drainage

16 Groundwater level

17 Haze

18 Fire

19 Southeast Asia

20

21

22 **Abstract**

23 Tropical peat swamp forests have been experiencing drastic disturbances, such as  
24 deforestation, drainage, and fire. We examined how such disturbances influence albedo,  
25 which regulates radiative energy exchange between the terrestrial surface and the  
26 atmosphere. We conducted continuous field observations at three sites: undrained forest  
27 (UF), drained forest (DF), and drained burned ex-forest (DB), in Central Kalimantan,  
28 Indonesia, for over 13 years.

29 Observed albedo was strongly influenced by haze caused by fire because the haze  
30 layer covering the canopy has a relatively high reflectance. Under severe haze  
31 conditions in October 2015, apparent albedo increased to 0.156, 0.162, and 0.183 at the  
32 UF, DF, and DB sites respectively. Mean monthly albedos excluding fire periods were  
33  $0.094 \pm 0.005$ ,  $0.092 \pm 0.006$ , and  $0.099 \pm 0.017$  (mean  $\pm$  1 standard deviation) at the  
34 UF, DF, and DB sites respectively. Seasonal fluctuation in albedo at the DB site, where  
35 ferns were dominant, was greater than at the UF and DF sites.

36 Albedo at the DF site was significantly lower than that at the UF site from February  
37 to August ( $p < 0.05$ ). At the forest sites the albedo increased as groundwater level  
38 decreased. Albedo was higher under high vapor pressure deficit at all sites. At the DB  
39 site albedo decreased when the soil surface was water-saturated and patched with  
40 puddles, potentially due to the low albedo of open water. The albedo at the DB site was  
41 lower than that at the forest sites at the beginning of the observation period.  
42 Subsequently, the albedo increased and exceeded those at the UF and DF sites  
43 immediately after fire damage in 2009. This could be explained by the expansion of  
44 bright-colored ferns and sedges over dark-colored peat soil. According to our results,  
45 haze, groundwater level, and vegetation cover significantly influence albedo in tropical

46 peat swamp forests.

47

48

## 49 **1. Introduction**

50 Tropical peatlands sequester 105 Gt of soil organic carbon, accounting for 21% of the  
51 global peat carbon reserves, and are a major carbon reservoir (Page et al., 2011; Dargie  
52 et al., 2017). A significant portion of tropical peat, accounting for approximately 43% of  
53 all the tropical peat areas, occurs in Southeast Asia. The environments in numerous  
54 tropical peatlands in the region have changed due to the conversion of land, mainly into  
55 oil palm and acacia plantations (Miettinen et al., 2016). Drainages is often undertaken to  
56 lower the groundwater level (GWL) to facilitate agricultural activities. Consequently,  
57 soil aridification occurs, and fire risks increase in the dry season, since dry peat is  
58 highly combustible.

59 The Mega Rice Project (MRP) represents a case where a tropical peatland ecosystem  
60 has been degraded (Hoscilo et al., 2011). This project was launched in Central  
61 Kalimantan, Indonesia in 1996 to transform a vast peat swamp forest area into farmland,  
62 mainly rice fields. However, the MRP was officially canceled in 1999 mainly because of  
63 a prevailing economic crisis, leaving behind an abandoned peatland (Rieley and  
64 Muhmad, 2002). Consequently, more than 60% of the peat swamp forest in the MRP  
65 area disappeared from 1997 to 2000 (Page et al., 2009). In addition, in recent decades,  
66 oil palm has attracted the attention of farmers as a profitable cash crop. Consequently,  
67 oil palm plantations have expanded rapidly in recent times, especially in Southeast Asia.  
68 For example, in Kalimantan, 206,400 ha of peat swamp forest, equivalent to 3.8% of all  
69 Kalimantan swamp were converted into oil palm plantations by 2010 (Gunarso et al.,

70 2013).

71 Numerous studies on tropical peatlands have evaluated the effects of peatland  
72 disturbance on carbon dioxide (CO<sub>2</sub>) dynamics from a global warming perspective (e.g.,  
73 Page et al., 2002; Hirano et al., 2012; Itoh et al., 2017; Warren et al., 2017). Drainage of  
74 peatlands, which creates aerobic conditions in the environments, stimulates the  
75 degradation of peat via microbial activity, which in turn increases CO<sub>2</sub> efflux from the  
76 soil to the atmosphere (e.g., Sundari et al., 2012; Hirano et al., 2014; Itoh et al., 2017).  
77 Drainage of peatlands also increases fire risk and accelerates fire propagation. Fire is a  
78 disturbance that contributes considerably to global warming. In recent decades tropical  
79 peatlands in Indonesia, particularly in Sumatra and Kalimantan, repeatedly experienced  
80 large-scale fires in El Niño years (1997, 2002, 2009, 2014, and 2015). Huijnen et al.  
81 (2016) noted that widespread forest and peatland fires burned over a large area of  
82 maritime Southeast Asia in September and October 2015. The CO<sub>2</sub> emission rate (11.3  
83 Tg CO<sub>2</sub> per day) in the region in September–October 2015 exceeded the fossil fuel CO<sub>2</sub>  
84 emissions from the European Union (EU28) (8.9 Tg CO<sub>2</sub> per day) for that period. The  
85 large-scale fires in the region emitted large amounts of smoke and caused a dense haze  
86 which spread out up to the Malay Peninsula and Borneo.

87 Energy balance between terrestrial surfaces and the atmosphere should be considered,  
88 in addition to greenhouse gas fluxes in the evolution of the impact of various  
89 disturbances on global warming. Sensible heat, which directly warms the atmosphere, is  
90 referred to as net radiation energy. Albedo and incoming solar radiation influence net  
91 radiation a great deal. For example, forestation in boreal peatlands caused positive net  
92 radiative forcing at one of four sites by decreasing albedo (Lohila et al., 2010),  
93 indicating that forestation does not necessarily mitigate global warming. Burakowski et

94 al. (2018) quantified the impact of deforestation on surface temperature in the Eastern  
95 United States using on-site data and a model. They reported that surface cooling due to  
96 increased albedo that was caused by deforestation was lower than 0.2°C in summer.  
97 Zhang et al. (2020) also assessed the contribution of reforestation to global warming by  
98 comparing data from six paired forest–grassland sites in temperate zones. They  
99 estimated that the albedo warming effect due to reforestation was, on average, 2.3°C.  
100 Both studies demonstrated that decreased albedo over forestlands causes surface  
101 warming.

102 Conversely, several studies have also reported that deforestation increases albedo. For  
103 example, Loarie et al. (2011) showed that deforestation increased albedo by 2.8% and  
104 flooding increased albedo due to the submergence of vegetation in South America.  
105 Oliveira et al. (2019) also demonstrated increases in albedo in pasture, agricultural land,  
106 and secondary forest following the land conversion from primary tropical forests in  
107 southwestern Amazonia. Sabajo et al. (2017) also concluded that albedo in intact forests  
108 was lower than in other types of land cover: clear-cut land, palm oil plantation, and  
109 rubber plantation in Sumatra. As for peatland, the above-canopy albedo in a burned  
110 swamp forest was significantly higher than that of an unburned swamp forest in Finland  
111 (Thompson et al., 2015). Kuusinen et al. (2013) reported that the albedo of a clear-cut  
112 area was higher than those of forests, excluding that of a birch forest in Finland.

113 Many studies have evaluated albedo over large areas using satellite products such as  
114 MODIS. For example, Li et al. (2015) showed a difference in albedo between forest and  
115 open land at the global scale. They revealed that forests have lower albedo than open  
116 land, especially in northern mid-latitudes in winter. In the tropical zone (20°S–20°N),  
117 however, the mean albedo difference between forest and open land was low when

118 compared with differences in the other latitudinal ranges. They also concluded that the  
119 cooling or warming effects of forests are mainly driven by evapotranspiration and  
120 albedo.

121 Satellite products are useful in acquiring large-scale data for target areas but there is  
122 still room for improvement with regard to precision and resolution. Oliveira et al.  
123 (2019) reported that satellite data overestimate albedo as compared to field data. In  
124 addition, He et al. (2014) reported that the estimated albedo depends on the type of  
125 satellite data employed. Cescatti et al. (2012) analyzed field data obtained from 53  
126 FLUXNET sites and found some mismatch between *in situ* measurements and those  
127 from satellite products, especially in grasslands and crop lands, largely due to spatial  
128 heterogeneity. Field observations could reveal the characteristics of albedo under  
129 different environmental conditions. However, only a few studies based on long-term  
130 field observations in tropical peatlands has been conducted (e.g., Hirano et al., 2015;  
131 Tang et al., 2019; Kiew et al., 2020). Considering rapidly expanding land conversion, it  
132 is very important to evaluate the albedo which would change significantly in tropical  
133 peatlands. Albedo affects not only radiation balance directly but also evapotranspiration  
134 through energy balance. Evapotranspiration is a key component in water balance and  
135 affects GWL, which governs oxidative peat decomposition. Thus, it is important to  
136 know how albedo changes following disturbance. In this study we measured  
137 meteorological variables, GWL and albedo at three tropical peat ecosystems under  
138 different degrees of disturbance, namely undrained forest (UF), drained forest (DF), and  
139 drained burned ex-forest (DB) in Central Kalimantan, Indonesia, for more than 13 years.  
140 By comparing the albedo responses to environmental variations we examined how the  
141 drainage and fire environmental disturbances influenced albedo.

142

143

144

## 145 **2. Materials and Methods**

### 146 **2.1. Site description**

147 The study area was in the upper catchment of the Sebangau river, approximately 20  
148 km south of Palangkaraya City in Central Kalimantan, Indonesia (Fig. 1). The area was  
149 partly within the western section (Block C) of the former Mega Rice Project (MRP).  
150 Fire frequently occurred during the dry season and the burnt area increased in size in El  
151 Niño periods including 2002–2003, 2004–2005, 2006–2007, 2009–2010, 2012, and  
152 2014–2016, as defined by NOAA  
153 (<https://www.ncdc.noaa.gov/teleconnections/enso/indicators/sst/>). In Central  
154 Kalimantan the dry season in normal years lasts for approximately three months,  
155 between July and October.

156 The UF, DF, and DB sites were located within 15 km of each other. UF site was a  
157 relatively intact forest, though it had been selectively logged until the late 1990s. DF  
158 site had also been selectively logged during the same period, and a large canal was  
159 excavated in 1996 and 1997. Although UF and DF sites were evergreen broad-leaved  
160 forests, some defoliation was seen, namely not all the leaves were fallen at the end of  
161 the dry season (Fig. 2). Hirano et al. (2007) reported that leaf area index (LAI) slightly  
162 decreased from October to December. The DB site was burned at least four times; in  
163 1997, 2002, 2009, and 2014. In 2009 sensors and cables on and under the ground were  
164 severely damaged by fire. After vegetation was burned in 2009, ferns rapidly grew and  
165 covered most of the soil surface. In September 2014 the density of young trees, mainly



166 *Combretocarpus rotundatus* (DBH > 3 cm) was 846 trees ha<sup>-1</sup>. The forest floor was  
167 uneven with hummocks and hollows at UF and DF site. Hummocks forming on dense  
168 tree roots are generally 20–30 cm higher than surrounding vegetation-free hollows. In  
169 contrast, no such microtopography was found in DB site, because hummocks were  
170 burned. Further information on the three sites is presented in Table 1 and described by  
171 Hirano et al. (2012).

172

## 173 **2.2. Measurement**

174 The variables used in the present study are listed in Table 2. Observations were  
175 conducted on towers from July 2004 to June 2017 at the UF site, from November 2001  
176 to June 2017 at the DF site, and from April 2004 to February 2017 at the DB site. Some  
177 of the data are listed in Table 1.

178 At the UF and DF sites, downward and upward shortwave radiations were measured  
179 using a radiometer (CNR-1; Kipp & Zonen, Delft, the Netherlands) at heights of 36.3  
180 and 40.6 m respectively. At the DB site the height of measurement was elevated twice  
181 owing to growth of vegetation (Table 1). Air temperature and relative humidity were  
182 measured using a platinum resistance thermometer and a capacitive hygrometer  
183 (HMP45; Vaisala, Helsinki, Finland) at heights of 36.3, 41.7, and 1.5 m at the UF, DF,  
184 and DB sites respectively, while precipitation was measured using a tipping-bucket rain  
185 gauge (TE525; Campbell Scientific Inc., Logan, UT, USA) at heights of 36.0, 41.0, and  
186 1.5 m at the UF, DF, and DB sites respectively.

187 Sensor signals were measured every 10 s and each 30-min average was logged with a  
188 datalogger (CR10X or CR1000; Campbell Scientific Inc.). Groundwater level (GWL),  
189 defined as the distance between the groundwater surface and the ground surface, was

190 measured half-hourly with a water level logger (DL/N; Sensor Technik Sirnach AG,  
191 Sirnach, Switzerland or DCX-22 VG; Keller AG, Winterthur, Switzerland) within 5 m  
192 from experimental towers at the three sites. Positive GWLs denote the water levels are  
193 aboveground, whereas negative GWLs denote the water levels are belowground. Hirano  
194 et al. (2012) provided additional information on measurements.

195

### 196 **2.3. Data processing**

197 We defined albedo using the following equation:

$$198 \text{ albedo} = S_u / S_d \quad (1)$$

199 where  $S_u$  is the upward shortwave radiation ( $\text{W m}^{-2}$ ) and  $S_d$  is the downward shortwave  
200 radiation ( $\text{W m}^{-2}$ ). We used half-hourly data from 10:00 to 14:00 to minimize the effects  
201 of solar altitude. Furthermore, data during rain and within an hour after rain events were  
202 excluded to eliminate the influence of raindrops on the dome of the radiometer.

203 As an index for fire scale around the experimental sites, monthly burned fraction  
204 (BF) data in each  $0.25^\circ$  grid cell were extracted from the Global Fire Emission Database  
205 (<https://globalfiredata.org/pages/data/>). The cell for the UF site (cell 1) was within  $2.25^\circ$ –  
206  $2.5^\circ\text{S}$  and  $113.75^\circ$ – $114^\circ\text{E}$  and the cells for the DF and DB sites (cell 2) were within  $2.25^\circ$ –  
207  $2.5^\circ\text{S}$  and  $114^\circ$ – $114.25^\circ\text{E}$ . The data were available up until the end of 2016. Albedo  
208 chiefly reflects the color and structure of the plant canopy covering the ground surface.  
209 The light reflectance of leaves is influenced by leaf moisture and generally increases  
210 with a decrease in moisture. We used GWL and vapor pressure deficit (hPa, VPD) as  
211 indices of pedospheric and atmospheric dryness. VPD was calculated based on the air  
212 temperature and relative humidity data at each site.

213 We used the aerosol optical depth (AOD) as a reference value for the degree of

214 attenuation of shortwave radiation by haze. AOD was measured with a photometer at a  
 215 height of 27 m at the Palangkaraya AERONET site (2.23°S, 113.95°E), which is  
 216 approximately 11 km north of the UF site and approximately 16 km northeast of the DF  
 217 and DB sites. The observations began on 19 July, 2012. The data were acquired from  
 218 the AERONET database ([https://aeronet.gsfc.nasa.gov/new\\_web/aerosols.html](https://aeronet.gsfc.nasa.gov/new_web/aerosols.html)). We  
 219 used the highest quality data categorized at level 2.0 (cloud cleared and quality assured).  
 220

#### 221 **2.4 Quantitative evaluation of the haze effect on albedo**

222 Frequent fires in the dry season cause haze and affect the atmospheric optical  
 223 environment, namely through transmission, scattering, and absorption of shortwave  
 224 radiation. We examined the haze effect quantitatively by calculating the increases or  
 225 decreases from the values under no-haze conditions. The haze layer between the  
 226 observation height ( $H_{obs}$ ) and canopy height ( $H_{cano}$ ) was used for calculations. We also  
 227 examined the validity of our directly measured albedo with radiometers by comparing  
 228 observed albedo and theoretically calculated albedo at the observation heights. To do  
 229 this (refer to Fig. 3), we defined the reflectance, absorbance, and transmittance of the  
 230 haze layer as  $\beta$ ,  $\gamma$ , and  $\lambda$  ( $\beta + \gamma + \lambda = 1$ ). Incoming  $S_d$  at  $H_{obs}$  is distributed into reflected  
 231 upward radiation at  $H_{obs}$  ( $\beta S_d$ ), absorbed radiation in the layer ( $\gamma S_d$ ), and transmitted  
 232 radiation to  $H_{cano}$  ( $\lambda S_d$ ). Defining albedo at the canopy as  $\alpha_{cano}$ ,  $\lambda S_d$  was reflected upward  
 233 as  $\alpha_{cano} \lambda S_d$ , and then attenuated through the haze layer and reached  $H_{obs}$  as  $\alpha_{cano} \lambda^2 S_d$ .  
 234 Therefore,  $S_u$  and albedo at  $H_{obs}$  ( $\alpha_{obs}$ ) are expressed as follows:

$$235 \quad S_u = \alpha_{cano} \lambda^2 S_d + \beta S_d \quad (2)$$

$$236 \quad \alpha_{obs} = \frac{S_u}{S_d} = \frac{\alpha_{cano} \lambda^2 S_d + \beta S_d}{S_d} = \alpha_{cano} \lambda^2 + \beta \quad (3)$$

237 Note that  $\lambda \approx 1$  and  $\beta \approx 0$  under no haze conditions because the distance between  $H_{obs}$   
238 and  $H_{cano}$  was relatively short (less than 15 m).

239 The transmittance  $\lambda$  was calculated using the Beer-Lambert Law, as follows:

$$240 \quad \lambda = \exp(-b_{ext}x_L) \quad (4)$$

241 where  $x_L$  is the distance between  $H_{obs}$  and  $H_{cano}$ , and  $b_{ext}$  is the extinction coefficient.

242 According to the results of laboratory experiments under daylight viewing conditions,

243  $\lambda=0.02$  is usually employed as the perceptible threshold for visual range calculations

244 (Seinfeld and Pandis, 2006). When  $\lambda=0.02$ , the visibility distance  $x_v$  can be evaluated

245 using the following equation (the Koschmeider equation):

$$246 \quad x_v = \frac{3.912}{b_{ext}} \quad (5)$$

247 To facilitate the comparison of the results of the present study with those of previous

248 studies we performed calculations under the most severe haze conditions with AOD = 3

249 for the DF site. According to Kusumaningtyas et al. (2016)  $x_v$  is shorter than 500 m at an

250 AOD of 3. Therefore,  $b_{ext}$  is calculated to be more than  $7.82 \times 10^{-3} \text{ m}^{-1}$ . In addition,

251 applying the distance  $x_L=14.6$  m between  $H_{obs}=40.6$  m and  $H_{cano}=26$  m at the DF site in

252 Eq. 4,  $\lambda$  is calculated to be lower than 0.89, which indicates that  $\beta+\gamma$  is greater than 0.11

253 ( $1 - 0.89 = 0.11$ ). According to Seinfeld and Pandis (2006), light scattering by particles

254 with sizes comparable to the wavelength of visible light is largely responsible for

255 visibility reduction in the atmosphere and scattering by particles accounts for 50–95%

256 of light extinction. In non-urban sites scattering and absorption account for 80–95% and

257 10–25% light extinction respectively. Assuming that backscattering radiation to the

258 atmosphere ( $\beta S_d$ ) is 80% of the extinction of  $S_d$  ( $\beta / (\beta + \gamma) = 0.80$ ),  $\beta$  is calculated as

259 0.086. The above equations and calculations will be used in the Discussion section.

260

### 261 **3. Results**

#### 262 **3.1 Overview of meteorological conditions**

263 Figure 4 presents a time series of monthly environmental variables from 2004 to 2017.  
264 Monthly precipitation ranged from 80, 82, and 82 mm in August to 341, 323, and 326  
265 mm in December on average in 2004–2016 at the UF, DF, and DB sites respectively.  
266 Similar seasonal variations in precipitation were seen at the all three sites, in which  
267 precipitation started to decrease in May until August then started to increase in  
268 September until November. Mean annual precipitation from 2005 to 2016 was  $2663 \pm$   
269  $479$ ,  $2623 \pm 479$ , and  $2641 \pm 473$  mm (mean  $\pm$  1 standard deviation) at the UF, DF, and  
270 DB sites respectively. Meanwhile, annual air temperature exhibited slight seasonal  
271 fluctuation with bimodal peaks in May and October. Mean annual air temperatures from  
272 2005 to 2016 were  $26.1 \pm 0.5$ ,  $26.1 \pm 0.2$ , and  $26.4 \pm 0.3$  °C at the UF, DF, and DB sites  
273 respectively. Variation in the GWL was synchronized with precipitation events. In the  
274 wet season, GWL became positive (aboveground) at the UF and DB sites whereas it  
275 remained negative (belowground) at the DF site. GWL at the DB site has decreased  
276 since 2014 due to the drainage channel excavation activities nearby.

277 Albedos at the UF and DF sites had been increasing slightly with occasional rises.  
278 Conversely, albedo at the DB site increased gradually, with seasonal fluctuation  
279 throughout the observation period. Monthly BF data in the two cells were almost  
280 synchronized, although cell 2 had a higher BF than cell 1. BF in cell 2 was the highest,  
281 at 0.10, in September 2009, when the DB site was damaged severely by fire.

282

#### 283 **3.2 Seasonal variation in albedo**

284 Figure 5 shows the monthly ensemble average of albedo at the three sites. Data plots  
285 were classified using BF. Albedo generally increased with an increase in BF in the dry  
286 season. Excluding the influence of haze ( $BF \geq 0.005$ ), monthly averages ranged from  
287 0.092 in May to 0.096 in December at the UF site, from 0.087 in April to 0.098 in  
288 December at the DF site, and from 0.087 in April to 0.109 in September at the DB site.  
289 The mean monthly albedo with  $BF < 0.005$  over the entire observation period was  $0.094$   
290  $\pm 0.005$ ,  $0.092 \pm 0.006$ , and  $0.099 \pm 0.017$  (mean  $\pm 1$  standard deviation) at the UF, DF,  
291 and DB sites respectively, excluding the data during fires. There were significant  
292 differences ( $p < 0.01$ ) of albedo at DB site with those at UF and DF sites from the whole  
293 study period. Figure 6 illustrates the inter-site differences in monthly albedo with 95%  
294 confidence intervals determined using the bootstrap method with 1000 repetitions. From  
295 February to August, the albedo at the DF site was significantly lower than that at the UF  
296 site ( $p < 0.05$ ). Albedo at the DB site was significantly greater ( $p < 0.05$ ) than the albedo at  
297 the UF site in July, September, and October, and that at the DF site from July to October.  
298 All monthly albedo values at each site are listed in the Appendix.

299

### 300 **3.3 Inter-annual variation in albedo**

301 Albedo at the DB site increased annually since observations began (Fig. 4c). At the  
302 end of 2016 the albedo recorded was 0.131, exceeding those at the UF and DF sites by  
303 more than 0.02. Figure 7 illustrates the inter-annual variation in albedo at the three sites.  
304 Annual increments in albedo were calculated by applying linear regression to the data  
305 only in April–June to eliminate the influence of fire and to use the entire datasets at all  
306 the sites. BF in April–June was below 0.005 throughout the observation period (Fig. 7).  
307 The increasing rate at the DB site was the highest ( $0.0044 \text{ year}^{-1}$ ,  $R^2 = 0.76$ ,  $p < 0.01$ ),

308 followed by the DF site ( $0.0013 \text{ year}^{-1}$ ,  $R^2 = 0.74$ ,  $p < 0.01$ ) and UF site ( $0.0007 \text{ year}^{-1}$ ,  
309  $R^2 = 0.50$ ,  $p < 0.01$ ).

310

### 311 **3.4 Influence of environmental conditions**

312 Generally, the timing of positive peaks of albedo in the dry season corresponded to  
313 negative peaks of GWL and positive peaks of BF and AOD, especially in 2006, 2009,  
314 and 2015 (Fig. 4b–e). In 2015 the maximum albedo levels were 0.156, 0.162, and 0.183  
315 at the UF, DF, and DB sites, respectively. In addition, BF had positive peaks of 0.042 in  
316 cell 1 and 0.087 in cell 2, and AOD reached 3.79. In contrast, although BF and AOD  
317 had their positive spikes in 2012, no clear sharp spikes of albedo were observed.

318 The influence of water conditions on light reflection characteristics was examined.  
319 The relationship between albedo and GWL is illustrated in Figure 8. Daily average data  
320 were classified by AOD. High albedo (below around  $-1.0 \text{ m}$ ) was observed at low GWL  
321 ranges at all sites. Generally, albedo increased with an increase in AOD. Some plots  
322 with  $\text{AOD} \geq 0.5$  were also observed at relatively high GWLs from September to  
323 October 2012, during which time GWL did not decrease markedly, while AOD peaked  
324 (Fig. 4). Excluding the  $\text{AOD} \geq 0.5$  data, albedo showed a significant negative  
325 relationship with GWL at the UF and DF sites. Conversely, the albedo at the DB site  
326 was not significantly correlated with GWL when  $\text{GWL} < 0 \text{ m}$ . When groundwater rose  
327 aboveground ( $\text{GWL} \geq 0 \text{ m}$ ), albedo seemed to be lower than the estimated value by the  
328 fitted line for  $\text{GWL} < 0$  at the DB site but not at the UF site.

329 Figure 9 illustrates the relationship between albedo and VPD. Data with  $\text{AOD} \geq 1.0$   
330 were generally greater than data with  $\text{AOD} < 0.5$ . Albedo increased slightly at the  
331 lowest and highest VPD ranges ( $\text{VPD} < \text{ca.}10$  and  $\text{VPD} \geq \text{ca.}25 \text{ hPa}$ ) at the UF and DF

332 sites. For the  $AOD < 0.5$  data, the quadratic relationships were significant ( $p < 0.05$ ). On  
333 the other hand, linear and quadratic fittings were roughly overlapped each other and  
334 both fitting lines showed increasing trend of albedo with VPD within the observed  
335 range at DB site.

336

337

## 338 **4. Discussion**

### 339 **4.1 Comparison with other studies**

340 Table 3 provides a range of literature values from this study and previous studies. The  
341 mean observed albedo values (0.092–0.099) at  $BF < 0.005$  at the sites were lower than  
342 those in other tropical forests: 0.114–0.12 in an Amazonia forest (Cescatti et al., 2012;  
343 Oliveira et al., 2019). Peat swamp forests might have canopy structures similar to those  
344 of Amazonian forests, forming dense crown canopies of evergreen broadleaf trees.  
345 However, in our study area a few small canopy gaps were generated by tree fall  
346 especially at the DF site. The reduction in upward reflection due to the resulting uneven  
347 canopy could be the reason for the lower albedo at our forest sites. In addition, the  
348 albedo observed in the present study was much lower than that in treeless peatlands:  
349 0.132 at a Finnish peat bog in summer (Gao et al., 2014); 0.137 at an open mesotrophic  
350 fen on a Finnish peat soil in July (Lohila et al., 2010); and 0.140 at an open Finnish  
351 peatland in summer (Kuusinen et al., 2013). Bright-colored short vegetation dominating  
352 the ground surface could be the reason for the higher albedo in treeless peatlands.

353

### 354 **4.2 Influence of land cover change**

355 Compared with that at the forest sites (UF and DF), albedo at the burned site (DB)



356 was higher after a severe fire in 2009, when the ground was mostly covered with  
357 vegetation mainly comprising ferns (Fig. 4c). Many studies have reported an increasing  
358 albedo following deforestation in the tropics. For example, albedo increased by 0.027  
359 and 0.032 following the conversion of tropical forests into pasture and agricultural land  
360 respectively in southwestern Amazonia (Oliveira et al., 2019). Berbet and Costa (2003)  
361 reported that the albedo increased by 0.043 following the replacement of a tropical  
362 forest with pasture in Amazonia. In addition, Sabajo et al. (2017) reported that the  
363 albedo of clear-cut areas was 0.02 higher than that of forests in Sumatra, Indonesia.  
364 However, the albedo of the DB site was lower than those of the UF and DF sites until  
365 the middle of 2009 (Fig. 4c), potentially because relatively dark colored bare peat was  
366 still largely exposed. In contrast, Thompson et al. (2015) reported that albedo at a  
367 burned peat bog was higher than that at an unburned site over a two-year period  
368 following a wildfire, with no clear difference detected after four years. They explained  
369 that the higher albedo at the burned site was due to the immediate recovery of  
370 *Sphagnum* moss over the peat soil.

371 The albedo of the DB site exhibited an increasing trend up to 0.131 at an annual rate  
372 of  $0.0044 \text{ year}^{-1}$  until 2016 (Fig. 7c). An increase in albedo after fire, which represented  
373 a 0.08 increase over the first decade, was also observed in burned boreal forests (Amiro  
374 et al., 2006). The albedo of 0.131 was generally lower than that observed in shrubland,  
375 savanna, grassland, and cropland (e.g., Myhre et al., 2005; He et al., 2018; Ge et al.,  
376 2019). The comparison of albedo at DB site with those at reference sites mentioned  
377 above and Figure 7c suggest that albedo continued to increase at the DB site as long as  
378 the existing light-colored herbaceous plants was expanding. Page et al. (2009) reported  
379 that a high-intensity fire prevents transition of non-forest vegetation or bare peat into

380 forest and replaces the plant community with ferns and sedges with few or no trees.  
381 Over the last few decades, fire has occurred so frequently that DB sites have become  
382 dominated by ferns and no change in this condition is expected. Therefore, observations  
383 at short term intervals are essential to capture such dynamic variation and to make  
384 precise estimates of albedo.

385 The annual albedo of forest sites has also been increasing gradually (Fig. 7), although  
386 the annual rates of  $0.0007 \text{ year}^{-1}$  at the UF site and  $0.0013 \text{ year}^{-1}$  at the DF site were  
387 lower than 30% of the rate observed at the DB site. Increasing albedo could reflect  
388 subtle changes in canopy structure with gradual tree growth. For example, canopy gaps  
389 were changing following the termination of selective logging in the late 1990s. Tree  
390 growth resulting in filling of canopy gaps would smooth the forest canopy and thus,  
391 increase albedo. Canopy recovery after tower construction might be another reason for  
392 the inter-annual increase.

393

#### 394 **4.3 Seasonal variation in albedo**

395 The larger seasonal fluctuation in albedo observed at the DB site as compared with  
396 the fluctuations at the UF and DF sites (Figs. 4 and 5) could be due to the greater  
397 seasonal fluctuation in ground conditions at the DB site, including exposure of peat soil  
398 and growth of ferns. The bare ground at the DB site, was much more exposed due to  
399 sparsely distributed vegetation. Basically, peat soil turns dark in the wet season and light  
400 in the dry season, depending on the GWL. At the UF and DF sites, however, the ground  
401 surface was almost entirely covered by a dense canopy. In addition, ferns dominating  
402 the DB site lightened leaf color in the dry season because of the decrease of leaf water  
403 content. Therefore, the albedo at the DB site increased in the dry season.

404 The annual amplitudes of albedo at the forest sites (0.004 at the UF site and 0.011 at  
405 the DF site, on average) were lower than those at other tropical forests (0.025; Berbet  
406 and Costa, 2003). The larger annual amplitudes were due to decreasing LAI in the dry  
407 period, resulting in higher albedo. Myneni et al. (2007) reported that the Amazon  
408 rainforest exhibits notable LAI seasonality with an annual amplitude of 25%. Our  
409 smaller annual range would indicate weaker LAI phenology.

410

#### 411 **4.4 Influence of fire smoke**

412 The AOD was similar in magnitude and seasonal variation to those in Amazonian  
413 forests. Oliveira et al. (2007) reported that AOD exceeded 3.0 during the dry season due  
414 to biomass burning events. Schafer et al. (2008) showed that AOD at 440 nm peaked in  
415 the dry season when fire occurred. Generally, AOD is a reliable index for fire smoke.

416 To examine the reliability of the albedo data measured directly with radiometers  
417 under the most severe haze conditions in the present study with an AOD of 3 at the DF  
418 site, we calculated  $\alpha_{obs}$  using Eq. 3 for comparison with the observed  $\alpha_{obs}$ . By assuming  
419  $\alpha_{obs} \approx \alpha_{cano}$  at  $BF < 0.005$  and applying the mean albedo (0.092) for  $\alpha_{cano}$  with  $\beta = 0.086$   
420 and  $\lambda = 0.89$  to Eq. 3,  $\alpha_{obs}$  was calculated to be 0.160. This value was comparable to the  
421 observed values ( $0.14 \pm 0.02$ , mean  $\pm 1$  standard deviation) at  $AOD \geq 3$  in Figs. 8b and  
422 9b;  $\alpha_{obs}$  is 174 % of  $\alpha_{cano}$ . That is, 74 % of overestimation was caused by haze. When  $x_v$   
423 is a half (250 m) or double (1000 m) the distance of 500 m,  $\alpha_{obs}$  is calculated to be 0.221  
424 and 0.126, respectively. Similarly, when  $x_L$  is a half (7.3 m) or double (29.2 m) the  
425 actual distance (14.6 m),  $\alpha_{obs}$  is calculated to be 0.126 and 0.221 respectively, with  $x_v =$   
426 500 m.

427 The calculated values above clearly indicate that severe haze causes the

428 overestimation of surface albedo and that albedo strongly depends on the distance  
429 between the observation height and the vegetation height. Therefore, distinctly high  
430 albedo during fire events must have resulted from the haze layers below the radiometer  
431 and not from sharp responses of vegetation. It is quite challenging to determine canopy  
432 albedo using single-point observations above the canopy under severe haze conditions.  
433 The degree of the haze effect on albedo was quantitatively demonstrated using  
434 equations 2 and 3.

435

#### 436 **4.5 The response of albedo to GWL and VPD**

437 First, we explain the variation in GWL at the DB site because GWL remained high  
438 until 2014 despite the drainage. The high GWL was partly caused by ground lowering  
439 due to the loss of surface peat by repeated fires. For example, surface peat was burned  
440 by 0.22 m in thickness in 2002 at DB site (Hirano et al., 2014). Another reason for the  
441 high GWL would be lower evapotranspiration due to low tree density (Hirano et al.,  
442 2015). However, GWL has decreased since 2014 because of channel excavation nearby.

443 Albedo clearly decreased at the DB site when GWL was positive (Fig. 8). Generally,  
444 the albedo of open water is lower than that of soil. Thus, the appearance of open water  
445 on the ground surface at the DB site, where some small puddles were exposed to the sky  
446 in the wet season, could have contributed to the decrease in albedo. In contrast, such a  
447 decrease in albedo was not observed even during flooding at the UF site because the soil  
448 surface was mostly covered with canopy. Loarie et al. (2011) reported a similar result,  
449 where flooding decreased forest albedo in South America.

450 In the forest sites in the present study, defoliation increased slightly in October–  
451 December (data not shown). In addition negative GWL peaks were regularly observed

452 in September–October. Leaf color turns brighter due to drying during the dry season  
453 with a slight corresponding decrease in LAI. Therefore, albedo had a negative  
454 relationship with GWL (Fig. 8) at the UF and DF sites. Sanchez-Mejia et al. (2014)  
455 have also investigated the relationship between albedo and GWL in a semiarid  
456 shrubland. They reported that albedo increased by about 0.03 in a closed canopy site  
457 and by about 0.05 in an open site with a lowering of GWL 0 to  $-0.6$  m. The rates of  
458 increase are higher than those observed at our sites: 0.006 (UF), 0.005 (DF), and 0.001  
459 (DB), following the lowering of GWL by 0.6 m (Fig. 8).

460 An increase in albedo with a lowering of GWL seems to be inconsistent as in this  
461 study in which the albedo at the DF site was not greater than that at the UF site.  
462 Although the differences between the UF and DF sites in canopy structure, tree species  
463 and phenology are potential reasons for the discrepancy, further investigations are  
464 required to establish robust evidence to explain this inconsistency.

465 In the present study the albedo increased at the lowest VPD range ( $VPD < ca. 10$  hPa)  
466 at the UF and DF sites. Water droplet might increase reflection of incoming solar  
467 radiation. Some water droplets might have remained on the leaf surfaces at the UF and  
468 DF sites even more than an hour after the rainfall under low VPD conditions whereas  
469 water droplets easily evaporated at the DB site. This could be because of the difference  
470 in vegetation height and structure between the forest and burned sites. Conversely,  
471 albedo increased at the highest VPD range ( $VPD \geq ca. 25$  hPa) at all three sites,  
472 potentially because leaf surfaces become lighter and reflection on leaf surfaces is  
473 enhanced to facilitate adaptation to water deficit under dry atmospheric conditions (e.g.,  
474 Yu et al., 2000). Therefore, changes in pedospheric and atmospheric moisture (or  
475 dryness) influenced albedo via vegetation responses, especially those of leaves.

476

477

## 478 **5. Conclusions**

479 Our continuous long-term field observations revealed the impact of fire and water  
480 conditions (GWL and VPD) on albedo in tropical peat ecosystems. Fire decreased land  
481 surface albedo by exposing the dark-colored peat soil. Subsequently, ferns regenerated  
482 immediately and expanded over the ground surface. Conversely, intensive fire  
483 sometimes caused severe haze. Apparent albedo sharply increased under such hazy  
484 conditions because the haze layer between the radiometer and canopy increased  
485 reflection of incoming downward radiation. Hence, the albedo of vegetation cannot be  
486 measured under such hazy conditions. Nevertheless, decreasing GWL slightly increased  
487 the albedo in both the undrained and drained forests. At the highest VPD range  
488 ( $VPD \geq ca. 25$  hPa), the albedo increased at all sites. Therefore, both pedospheric and  
489 atmospheric dryness increased albedo. When the soil surface was water-saturated (GWL  
490  $\geq 0$  m), albedo at the burned site decreased because the ground was dotted with exposed  
491 puddles. In contrast, no decrease was observed in the undrained forest because open  
492 water with low albedo was covered by the forest canopy.

493 We observed several environmental changes in response to rapidly shifting land  
494 surface characteristics. Therefore, short-interval measurements are required for the  
495 accurate evaluation of change in albedo. Our study also explored changes in albedo  
496 under heterogeneous environments. The expansion of the target area to the entire  
497 Southeast Asia and observation of trends under diverse meteorological conditions over  
498 different land cover types, including oil palm and acacia plantations, would be insightful.  
499 In addition, long-term continuous field observations before and after land conversion

500 would reveal impacts with a high temporal resolution.

501

502

503 **Acknowledgements**

504 This study was supported by JSPS Core University Program, JSPS KAKENHI Grant  
505 Numbers 13375011, 1525001, 21255001, 25257401, and 19H05666, the JST-JICA  
506 Project (SATREPS) (Wild Fire and Carbon Management in Peat-Forest in Indonesia)  
507 and Technology Development Fund (no. 2-1504) by the Environmental Restoration and  
508 Conservation Agency and the Ministry of the Environment, Japan. We are grateful to the  
509 late Dr. Suwido Limin for the site establishment. We also express our gratitude to the  
510 providers of burned fraction datasets of GFED, and Drs. Herizal, Catur Winarti, and  
511 Davis Setyo Nugroho for their efforts in establishing and maintaining the Palangkaraya  
512 AERONET site and for provision of data.

513

514

515

516 **References**

- 517 Amiro, B.D., Orchansky, A.L., Barr, A.G., Black, T.A., Chambers, S.D., Chapin, F.S.,  
518 Goulden, M.L., Litvak, M., Liu, H.P., McCaughey, J.H., McMillan, A., Randerson,  
519 J.T., 2006. The effect of post-fire stand age on the boreal forest energy balance. *Agric.*  
520 *For. Meteorol.* 140, 41–50. <https://doi.org/10.1016/j.agrformet.2006.02.014>.
- 521 Berbet, M.L.C., Costa, M.H., 2003. Climate change after tropical deforestation:  
522 seasonal variability of surface albedo and its effects on precipitation change. *J. Clim.*  
523 16, 2099–2104.  
524 [https://doi.org/10.1175/1520-0442\(2003\)016<2099:CCATDS>2.0.CO;2](https://doi.org/10.1175/1520-0442(2003)016<2099:CCATDS>2.0.CO;2).
- 525 Burakowski, E., Tawfik, A., Ouimette, A., Lepine, L., Novick, K., Ollinger, S., Zarzycki,  
526 C., Bonan, G., 2018. The role of surface roughness, albedo, and Bowen ratio on  
527 ecosystem energy balance in the Eastern United States. *Agric. For. Meteorol.* 249,  
528 367–376. <https://doi.org/10.1016/j.agrformet.2017.11.030>.
- 529 Cescatti, A., Marcolla, B., Vannan, S.K.S., Pan, J.Y., Román, M.O., Yang, X., Ciais, P.,  
530 Cook, R.B., Law, B.E., Matteucci, G., Migliavacca, M., Moors, E., Richardson, A.D.,  
531 Seufert, G., Schaaf, C.B., 2012. Intercomparison of MODIS albedo retrievals and in  
532 situ measurements across the global FLUXNET network. *Remote Sens. Environ.* 121,  
533 323–334. <https://doi.org/10.1016/j.rse.2012.02.019>.
- 534 Dargie, G.C., Lewis, S.L., Lawson, I.T., Mitchard, E.T.A., Page, S.E., Bocko, Y.E., Ifo,  
535 S.A., 2017. Age, extent and carbon storage of the central Congo Basin peatland  
536 complex. *Nature* 542, 86–90. <https://doi.org/10.1038/nature21048>.
- 537 Gao, Y., Markkanen, T., Backman, L., Henttonen, H.M., Pietikäinen, J.P., Mäkelä, H.M.,  
538 Laaksonen, A., 2014. Biogeophysical impacts of peatland forestation on regional



539 climate changes in Finland. *Biogeosciences* 11, 7251–7267.  
540 <https://doi.org/10.5194/bg-11-7251-2014>.

541 Ge, J., Pitman, A.J., Guo, W., Wang, S., Fu, C., 2019. Do uncertainties in the  
542 reconstruction of land cover affect the simulation of air temperature and rainfall in  
543 the CORDEX region of East Asia? *J. Geophys. Res. Atmos.* 124, 3647–3670.  
544 <https://doi.org/10.1029/2018JD029945>.

545 Gunarso, P., Hartoyo, M.E., Agus, F., Killeen, T.J., 2013. Oil palm and land use change  
546 in Indonesia, Malaysia and Papua New Guinea. Reports from the Technical Panels of  
547 the 2nd Greenhouse Gas Working Group of the Roundtable on Sustainable Palm Oil  
548 (RSPO) 29–64.

549 He, T., Liang, S., Song, D.X., 2014. Analysis of global land surface albedo climatology  
550 and spatial-temporal variation during 1981–2010 from multiple satellite products. *J.*  
551 *Geophys. Res. Atmos.* 119, 10,281–10,298. <https://doi.org/10.1002/2014JD021667>.

552 He, T., Liang, S., Wang, D., Cao, Y., Gao, F., Yu, Y., Feng, M., 2018. Evaluating land  
553 surface albedo estimation from Landsat MSS, TM, ETM+, and OLI data based on the  
554 unified direct estimation approach. *Remote Sens. Environ.* 204, 181–196.  
555 <https://doi.org/10.1016/j.rse.2017.10.031>.

556 Hirano, T., Segah, H., Kusin, K., Limin, S., Takahashi, H., Osaki, M., 2012. Effects of  
557 disturbances on the carbon balance of tropical peat swamp forests. *Global Change*  
558 *Biol.* 18, 3410–3422. <https://doi.org/10.1111/j.1365-2486.2012.02793.x>.

559 Hirano, T., Kusin, K., Limin, S., Osaki, M., 2014. Carbon dioxide emissions through  
560 oxidative peat decomposition on a burnt tropical peatland. *Global Change Biol.* 20,  
561 555–565. <https://doi.org/10.1111/gcb.12296>.

562 Hirano, T., Kusin, K., Limin, S., Osaki, M., 2015. Evapotranspiration of tropical peat

563 swamp forests. *Global Change Biol.* 21, 1914–1927.  
564 <https://doi.org/10.1111/gcb.12653>.

565 Hoscilo, A., Page, S.E., Tansey, K.J., Rieley, J.O., 2011. Effect of repeated fires on  
566 land-cover change on peatland in southern Central Kalimantan, Indonesia, from 1973  
567 to 2005. *Int. J. Wildland Fire* 20, 578–588. <https://doi.org/10.1071/WF10029>.

568 Huijnen, V., Wooster, M. J., Kaiser, J. W., Gaveau, D. L. A., Flemming, J., Parrington,  
569 M., Inness, A., Murdiyarso, D., Main, B., Weele, M., 2016. Fire carbon emissions  
570 over maritime Southeast Asia in 2015 largest since 1997. *Sci. Rep.* 6, 26,886.  
571 <https://doi.org/10.1038/srep26886>.

572 Itoh, M., Okimoto, Y., Hirano, T., Kusin, K., 2017. Factors affecting oxidative peat  
573 decomposition due to land use in tropical peat swamp forests in Indonesia. *Sci. Total*  
574 *Environ.* 609, 906–915. <https://doi.org/10.1016/j.scitotenv.2017.07.132>.

575 Kiew, K., Hirata, R., Hirano, T., Xhuan, W.G., Aries, E.B., Kemudang, K., Wenceslausa,  
576 J., San, L.K., Melling, L., 2020. Carbon dioxide balance of an oil palm plantation  
577 established on tropical peat. *Agric. For. Meteorol.* 295, 108189.  
578 <https://doi.org/10.1016/j.agrformet.2020.108189>

579 Kusumaningtyas, S.D.A., Aldrian, E., Rahman, M.A., Sopaheluwakan, A., 2016.  
580 Aerosol properties in central Kalimantan due to peatland fire. *Aerosol Air Qual. Res.*  
581 16, 2757–2767. <https://doi.org/10.4209/aaqr.2015.07.0451>.

582 Kuusinen, N., Tomppo, E., Berminger, F., 2013. Linear unmixing of MODIS albedo  
583 composites to infer subpixel land cover type albedos. *Int. J. Appl. Earth Obs.* 23,  
584 324–333. <https://doi.org/10.1016/j.jag.2012.10.005>.

585 Li, Y., Zhao, M., Motesharrei, S., Mu, Q., Kalnay, E., Li, S., 2015. Local cooling and  
586 warming effects of forests based on satellite observations, *Nat. Commun.* 6, 6603.  
587 <https://doi.org/10.1038/ncomms7603>.

588 Loarie, S.R., Lobell, D.B., Asner, G.P., Field, C.B., 2011. Land-Cover and Surface  
589 Water Change Drive Large Albedo Increases in South America, *Earth Interact.* 15, 1–  
590 16. <https://doi.org/10.1175/2010EI342.1>.

591 Lohila, A., Minkkinen, K., Laine, J., Savolainen, I., Tuovinen, J.P., Korhonen, L.,  
592 Laurila, T., Tietäväinen, H., Laaksonen, A., 2010. Forestation of boreal peatlands:  
593 impacts of changing albedo and greenhouse gas fluxes on radiative forcing. *J.*  
594 *Geophys. Res.* 115, G04011, <https://doi.org/10.1029/2010JG001327>.

595 Miettinen, J., Shi, C., Liew, S.C., 2016. Land cover distribution in the peatlands of  
596 Peninsular Malaysia, Sumatra and Borneo in 2015 with changes since 1990. *Glob.*  
597 *Ecol. Conserv.* 6, 67-78. <https://doi.org/10.1016/j.gecco.2016.02.004>.

598 Myhre, G., Kvalevag, M., Schaaf, C.B., 2005. Radiative forcing due to anthropogenic  
599 vegetation change based on MODIS surface albedo data, *Geophys. Res. Lett.* 32,  
600 L21410. <https://doi.org/10.1029/2005GL024004>.

601 Myneni, R.B., Yang, W., Nemani, R.R., Huete, A.R., Dickinson, R.E., Knyazikhin, Y.,  
602 Didan, K., Fu, R., Juárez, R.I.N., Saatchi, S.S., 2007. Large seasonal swings in leaf  
603 area of Amazon rainforests. *Proc. Natl. Acad. Sci. U.S.A.* 104 (12), 4820–4823.  
604 <https://doi.org/10.1073/pnas.0611338104>.

605 Oliveira, P.H.F., Artaxo, P., Pires, C., Lucca, S., Procopio, A., Holben, B., Schafer, J.,  
606 Cardoso, L.F., Wofsy, S.C., Rocha, H.R., 2007. The effects of biomass burning  
607 aerosols and clouds on the CO<sub>2</sub> flux in Amazonia. *Tellus B* 59, 338–349.  
608 <https://doi.org/10.1111/j.1600-0889.2007.00270.x>.

609 Oliveira, G., Brunzell, N.A., Moraes, E.C., Shimabukuro, Y.E., Santos, T.V., Randow, C.,  
610 Aguiar, R.G., Aragao, L.E.O.C., 2019. Effects of land-cover changes on the  
611 partitioning of surface energy and water fluxes in Amazonia using high-resolution  
612 satellite imagery. *Ecohydrology* 12, e2126. <https://doi.org/10.1002/eco.2126>.

613 Page, S., Hosięo, A., Wösten, H., Jauhainen, J., Silvius, M., Rieley, J., Ritzema, H.,  
614 Tansey, K., Graham, L., Vasander, H., Limin, S., 2009. Restoration ecology of  
615 lowland tropical peatlands in Southeast Asia: current knowledge and future research  
616 directions. *Ecosystems* 12, 888–905. <https://doi.org/10.1007/s10021-008-9216-2>.

617 Page, S.E., Siegert, F., Rieley, J.O., Boehm, H.D.O., Jaya, A., Limin, S., 2002. The  
618 amount of carbon released from peat and forest fires in Indonesia during 1997. *Nature*  
619 420, 61–65. <https://doi.org/10.1038/nature01131>.

620 Page, S.E., Rieley, J.O., Banks, C.J., 2011. Global and regional importance of the  
621 tropical peatland carbon pool. *Global Change Biol.* 17, 798–818.  
622 <https://doi.org/10.1111/j.1365-2486.2010.02279.x>.

623 Rieley, J., Muhamad, N.Z., 2002. Impact of inappropriate land use change on the peat  
624 swamps of Central Kalimantan. *Peatlands International* 1, 24–27.

625 Sabajo, C.R., Maire, G., June, T., Meijide1, A., Roupsard, O., Knohl, A., 2017.  
626 Expansion of oil palm and other cash crops causes an increase of the land surface  
627 temperature in the Jambi province in Indonesia. *Biogeosciences* 14, 4619–4635.  
628 <https://doi.org/10.5194/bg-14-4619-2017>.

629 Sanchez-Mejia, Z.M., Papuga, S.A., Swetish, J.B., van Leeuwen, W.J.D., Szutu, D.,  
630 Hartfield, K., 2014. Quantifying the influence of deep soil moisture on ecosystem  
631 albedo: The role of vegetation, *Water Resour. Res.* 50, 4038–4053.  
632 <https://doi.org/10.1002/2013WR014150>.

633 Schafer, J.S., Eck, T.F., Holben, B.N., Artaxo, P., Duarte, A.F., 2008. Characterization of  
634 the optical properties of atmospheric aerosols in Amazônia from long-term  
635 AERONET monitoring (1993–1995 and 1999–2006). *J. Geophys. Res.* 113, D04204,  
636 <https://doi.org/10.1029/2007JD009319>.

637 Seinfeld, J.H., Pandis, S.N. 2006. *Atmospheric Chemistry and Physics: From Air*  
638 *Pollution to Climate Change*. 2nd Edition, John Wiley & Sons, New York.

639 Sundari, S., Hirano, T., Yamada, H., Kusin, K., Limin, S., 2012. Effects of groundwater  
640 level on soil respiration in tropical peat swamp forests. *J. Agric. Meteorol.* 68, 121–  
641 134. <https://doi.org/10.2480/agrmet.68.2.6>.

642 Tang, A.C.I., Stoy, P.C., Hirata, R., Musin, K.K., Aries, E.B., Wenceslausa, J., Shimizu,  
643 M., Melling, L., 2019. The exchange of water and energy between a tropical peat  
644 forest and the atmosphere: Seasonal trends and comparison against other tropical  
645 rainforests. *Sci. Total Environ.* 683, 166–174.  
646 <https://doi.org/10.1016/j.scitotenv.2019.05.217>.

647 Thompson, D.K., Baisley, A.S., Waddington, J.M., 2015. Seasonal variation in albedo  
648 and radiation exchange between a burned and unburned forested peatland:  
649 implications for peatland evaporation. *Hydrol. Processes* 29, 3227–3235.  
650 <https://doi.org/10.1002/hyp.10436>.

651 Warren, M., Frolking, S., Dai, Z., Kurnianto, S., 2017. Impacts of land use, restoration,  
652 and climate change on tropical peat carbon stocks in the twenty-first century:  
653 implications for climate mitigation. *Mitig. Adapt. Strat. Gl.* 22, 1041–1061.  
654 <https://doi.org/10.1007/s11027-016-9712-1>.

655 Yu, G-R., Miwa, K., Nakayama, K., Matsuoka, N., Kon, H., 2000. A proposal for  
656 universal formulas for estimating leaf water status of herbaceous and woody plants

657 based on spectral reflectance properties. *Plant and Soil* 227, 47–58.

658 <https://doi.org/10.1023/A:1026556613082>.

659 Zhang, Q., Barnes, M., Benson, M., Burakowski, E., Oishi, A.C., Ouimette, A., Sanders-

660 DeMott, R., Stoy, P.C., Wenzel, M., Xiong, L., Yi, K., Novick, K.A., 2020.

661 Reforestation and surface cooling in temperate zones: mechanisms and implications.

662 *Global Change Biol.* 26, 3384–3401. <https://doi.org/10.1111/gcb.15069>.

663

664 **Figure legends**

665

666 Fig. 1 Map of the study area.

667 Fig. 2 Canopy photos of (a) UF, (b) DF and (c, d) DB sites.

668 Fig. 3 Schematic diagram of the partitioning of incoming shortwave radiation under  
669 severe haze conditions.

670 Fig. 4 Monthly variations in (a) precipitation, (b) GWL, (c) albedo, (d) BF, and (e)  
671 AOD. Precipitation shown in panel (a) was observed at the DF site. Month with  
672  $BF > 0.02$  in either cell was shown by shading in panel (b)-(e) as indicating fire  
673 event. Beginning month of canal construction in the vicinity of DB site is marked  
674 with an arrow in panel (b).

675 Fig. 5 Seasonal variations in monthly mean albedo at (a) UF, (b) DF, and (c) DB sites.  
676 Plots are classified into five categories by BF:  $BF < 0.005$ ,  $0.005 \leq BF < 0.01$ ,  
677  $0.01 \leq BF < 0.02$ ,  $0.02 < BF \leq 0.03$ , and  $0.03 \leq BF$ . The polyline connects the monthly  
678 average with  $BF < 0.005$ . Grey bars show the 95% confidence interval determined  
679 by a bootstrap method with 1000 replications.

680 Fig. 6 Inter-site differences in monthly albedo. The mean (plots) and 95% confidence  
681 interval (bars) were determined by the bootstrap method with 1000 replications.

682 Fig. 7 Inter-annual variation in albedo at (a) UF, (b) DF, and (c) DB sites. Monthly data  
683 for only April–June are shown to exclude the influence of fire.

684 Fig. 8 Relationship between albedo and GWL at (a) UF, (b) DF, and (c) DB sites. Plots  
685 were classified into five categories by AOD:  $AOD < 0.5$ ,  $0.5 \leq AOD < 1$ ,  $1 \leq AOD < 2$ ,  
686  $2 \leq AOD < 3$ , and  $3 \leq AOD$ . Data with  $AOD \geq 0.5$  in September–October 2012 were  
687 marked with crosses. A line was fitted to the data with  $AOD < 0.5$ . In panel (c),

688 line fitting was separately applied to two GWL ranges:  $GWL < 0$  and  $GWL \geq 0$ .

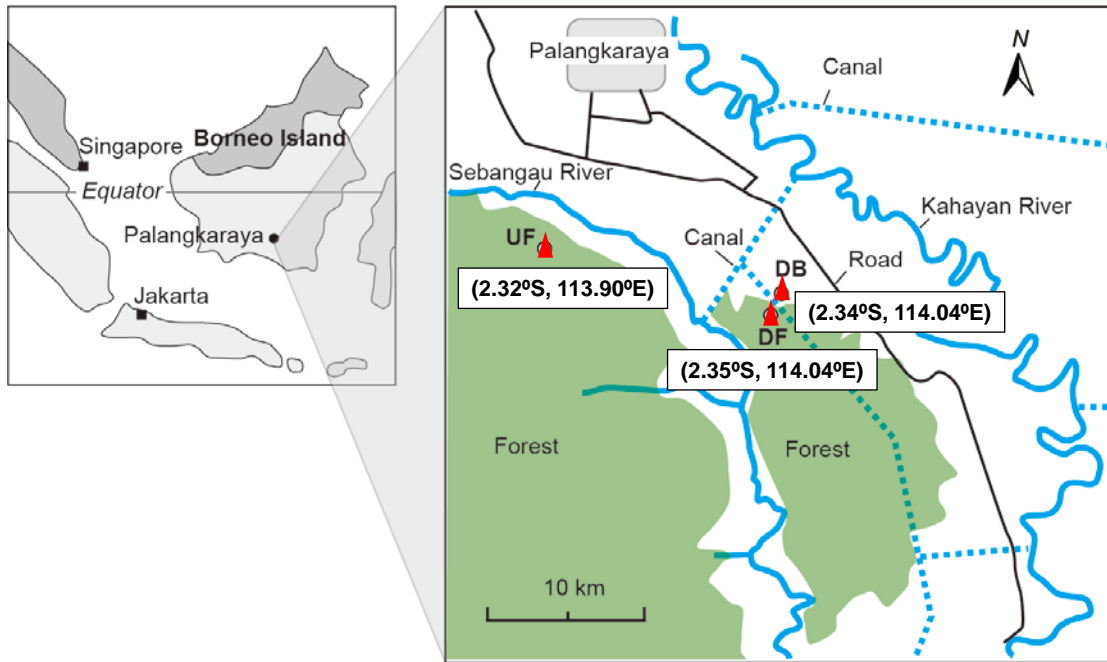
689 Fig. 9 Relationship between albedo and VPD at (a) UF, (b) DF, and (c) DB sites. Plots  
690 are classified into five categories by AOD, as shown in Fig. 8.

691

692



693 Figure 1



▲ : Location of observation towers

694

695

696 Figure 2

(a) UF site



(b) DF site



(c) DB site in a dry condition



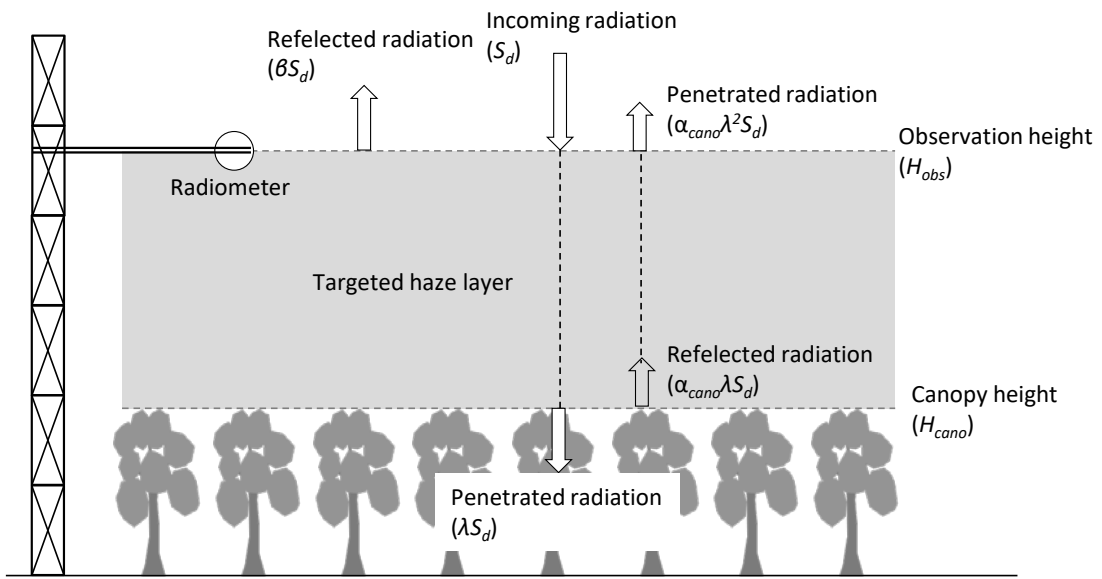
(d) DB site in a wet condition



697

698

699 Figure 3



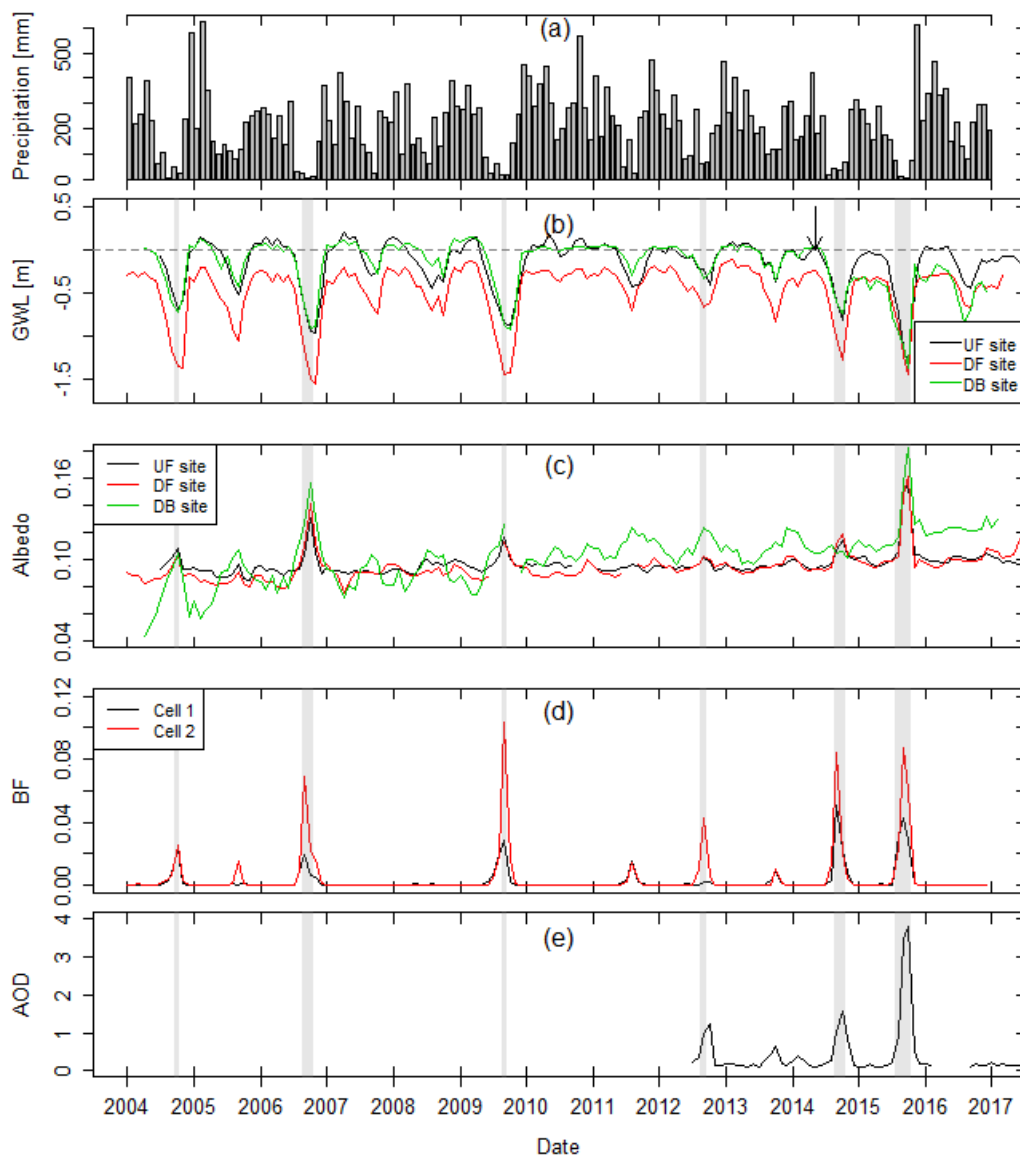
700

701

702

703 Figure 4

704



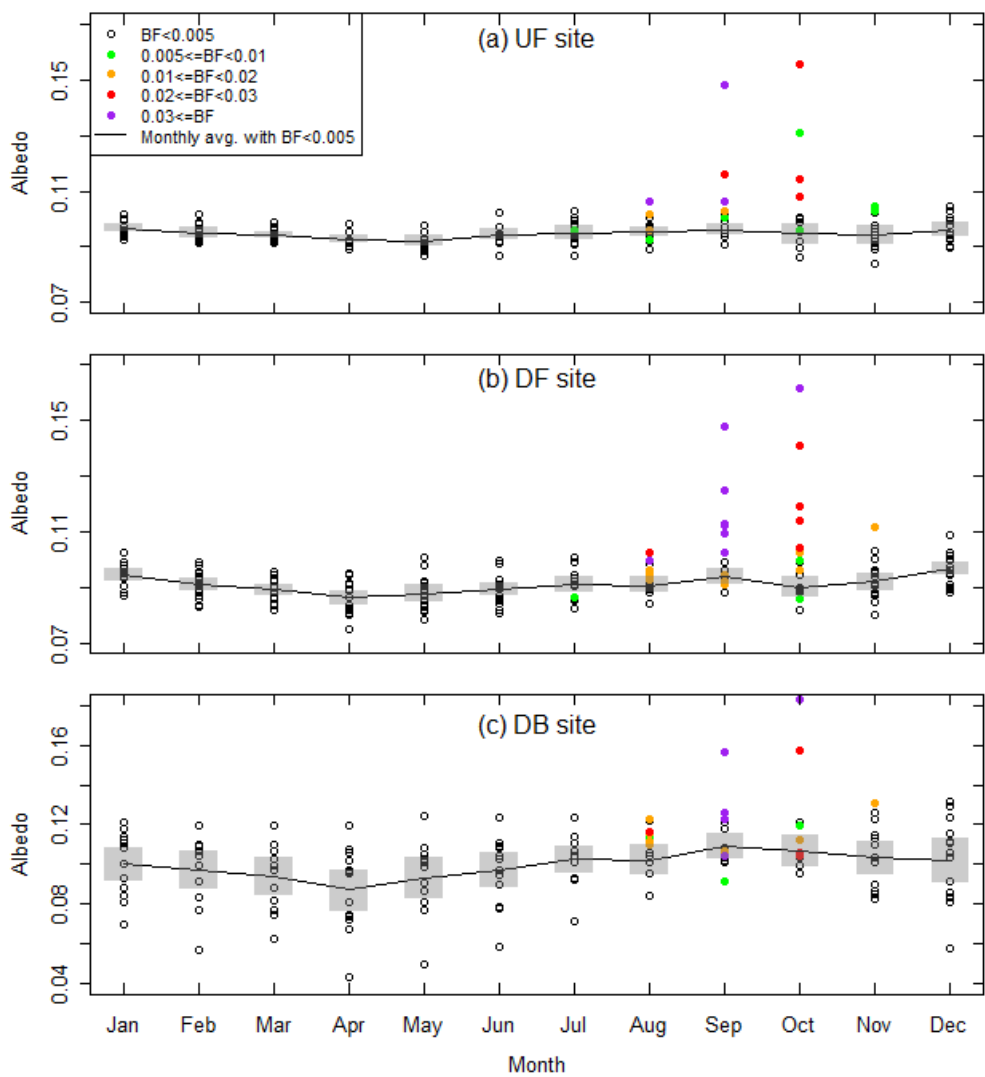
705

706

707

708 Figure 5

709



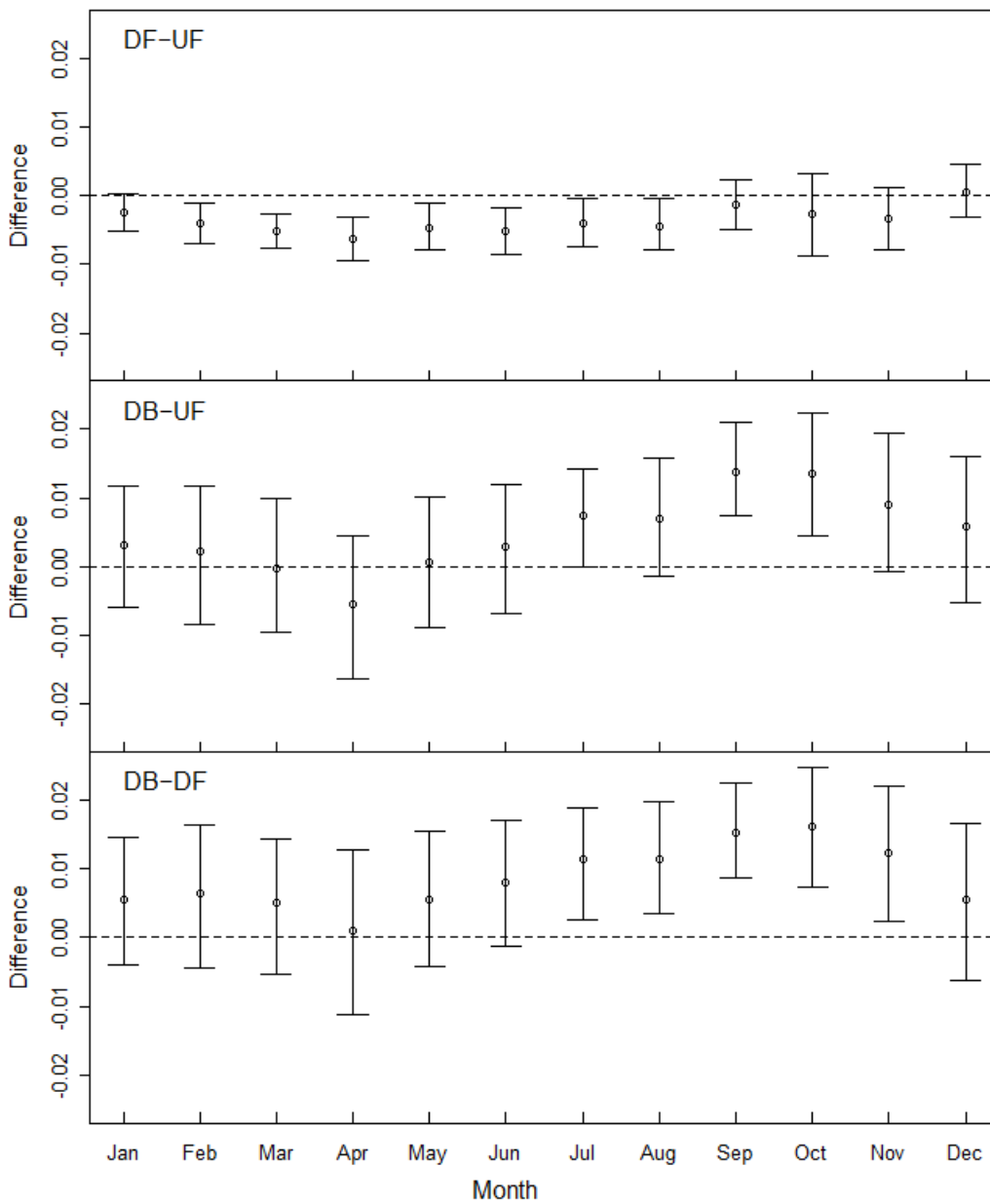
710

711

712

713 Figure 6

714

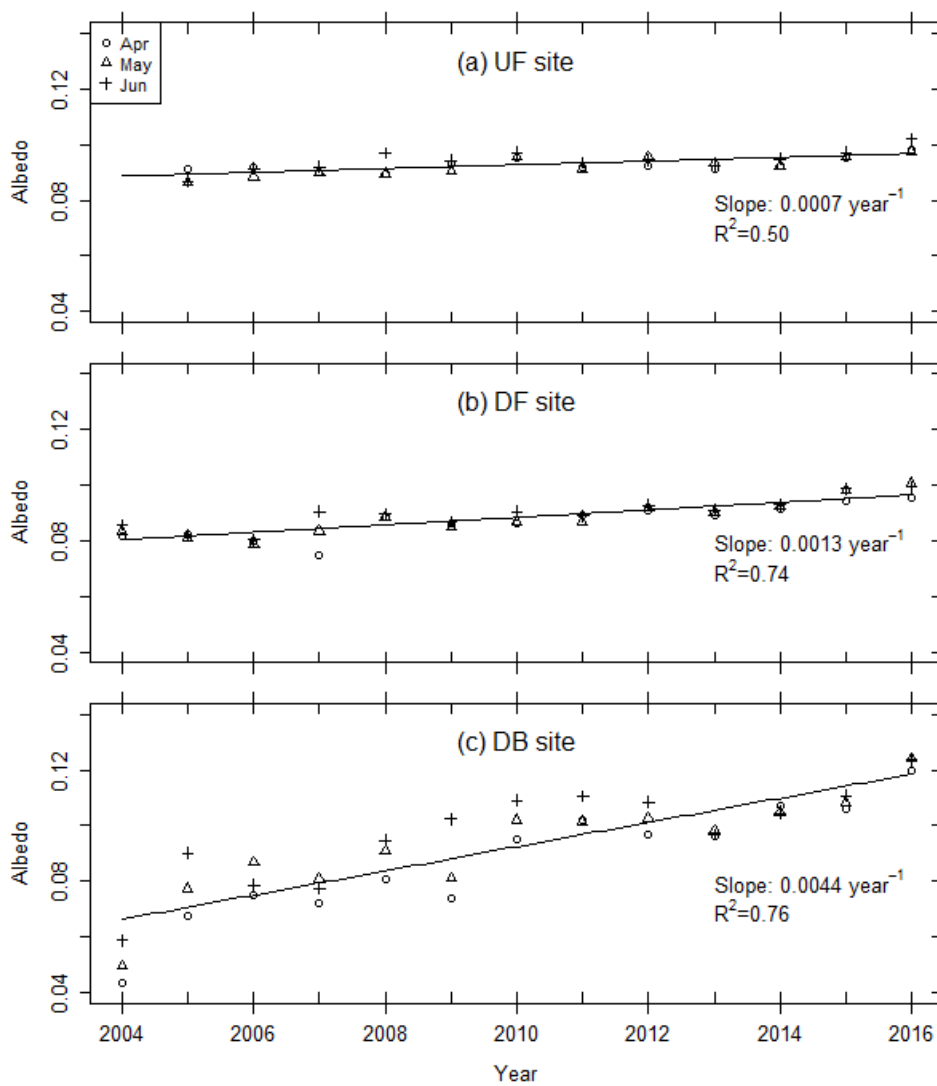


715

716

717 Figure 7

718



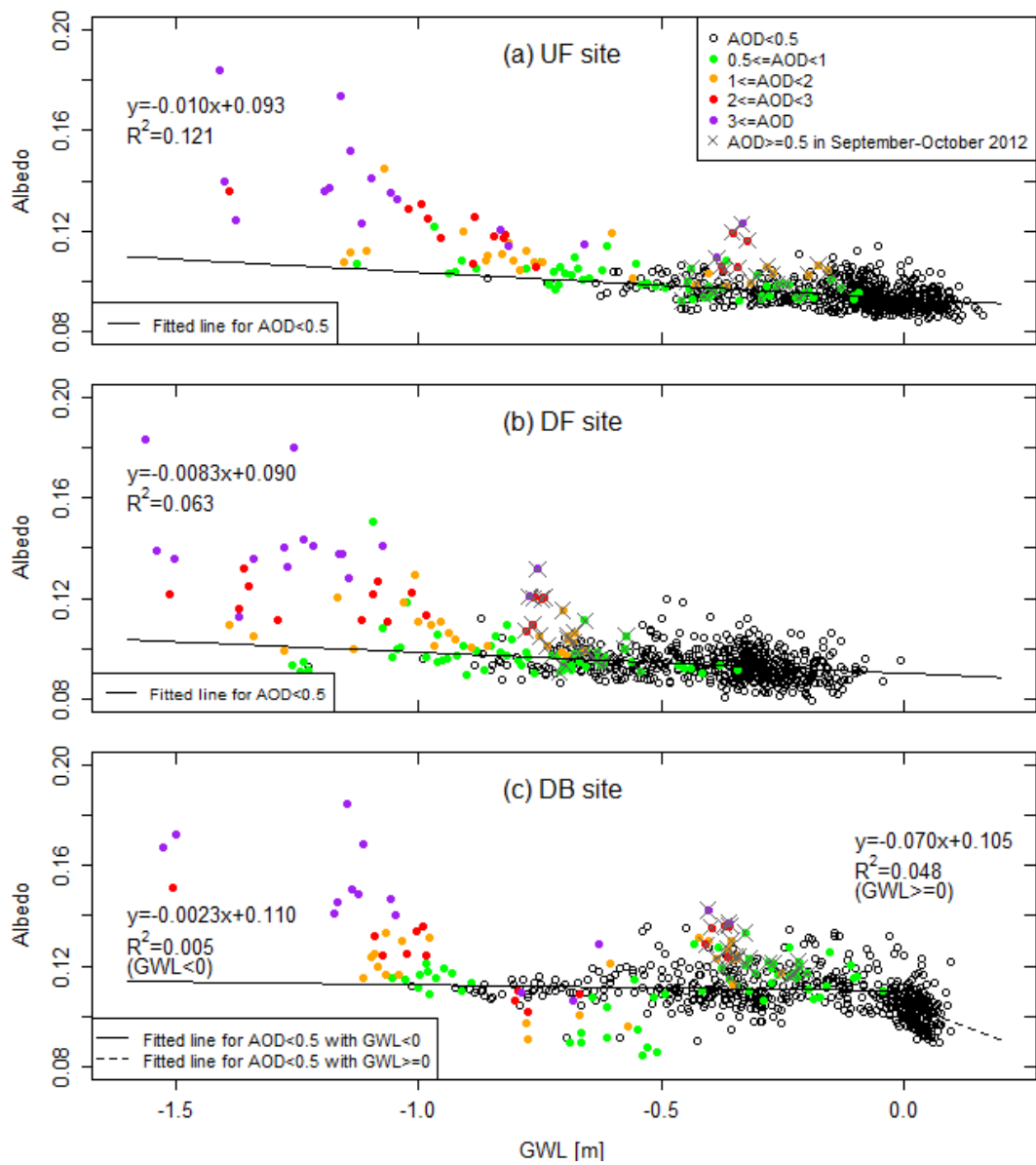
719

720

721

722 Figure 8

723



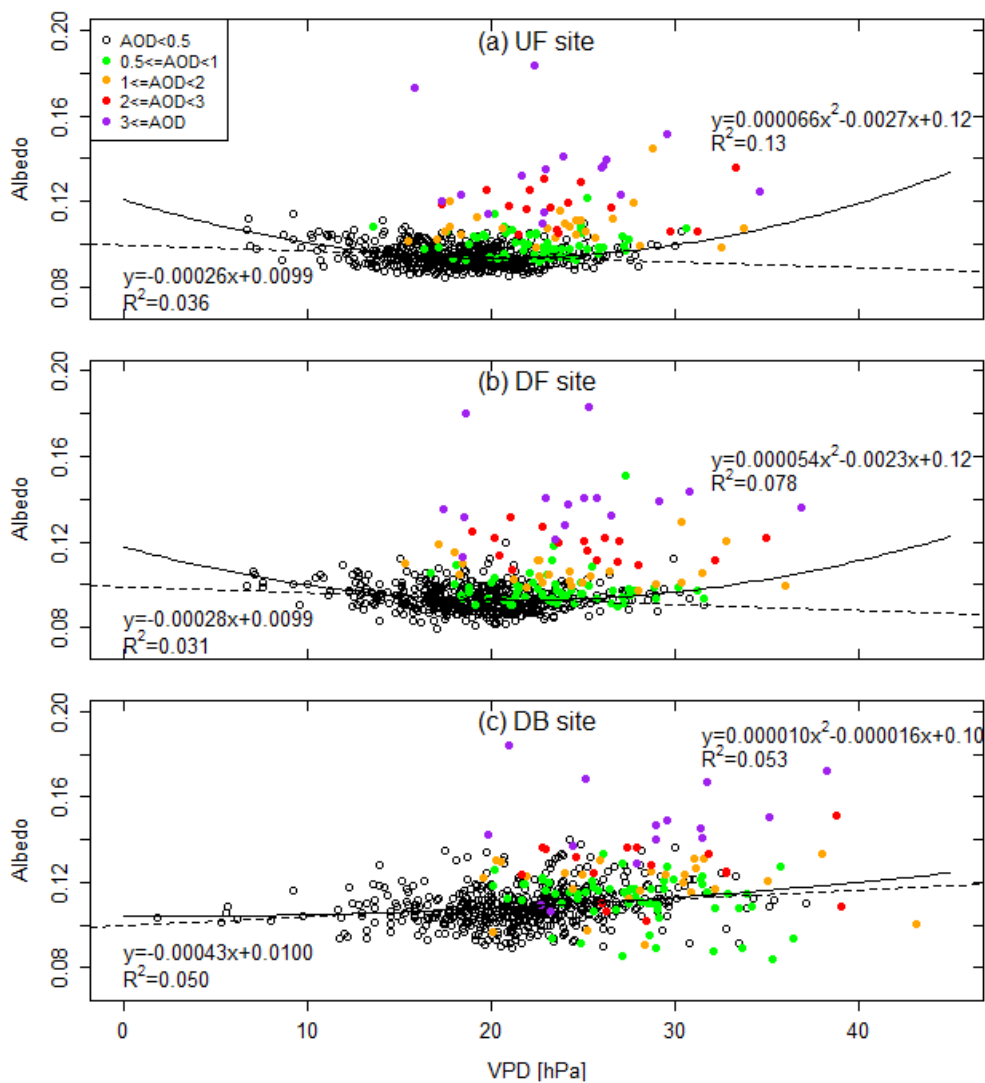
724

725



726 Figure 9

727



728

729

730

731 Table 1

732 Site information

733

| Site                   | UF                  | DF                      | DB                       |
|------------------------|---------------------|-------------------------|--------------------------|
| Geographical position  | 2.32°S, 113.90°E    | 2.35°S, 114.04°E        | 2.34°S, 114.04°E         |
| Observation period     | July 2004–June 2017 | November 2001–June 2017 | April 2004–February 2017 |
| Canopy height (m)      | 23                  | 26                      | 0.2–1.8                  |
| Radiometer             | 36.3                | 40.6                    | 3.3 (Apr 2004–Mar2012)   |
| measurement height (m) |                     |                         | 6.8 (Mar 2012–Dec 2013)  |
|                        |                     |                         | 13.6 (Dec 2013–Feb 2017) |
| Air temperature        | 36.0                | 41.7                    | 1.5                      |
| measurement height (m) |                     |                         |                          |

734

735 Table 2

736 Nomenclature

| Notation        | Unit       | Definition  |
|-----------------|------------|---|
| GWL             | m          | Groundwater level                                     |
| $S_u$           | $W m^{-2}$ | Upward shortwave radiation                            |
| $S_d$           | $W m^{-2}$ | Downward shortwave radiation                          |
| BF              |            | Burned fraction                                       |
| VPD             | hPa        | Vapor pressure deficit                                |
| AOD             |            | Aerosol optical depth                                 |
| $H_{obs}$       | m          | Observation height                                    |
| $H_{cano}$      | m          | Canopy height   |
| $\beta$         |            | Reflectance of the haze layer                         |
| $\gamma$        |            | Absorbance of the haze layer                          |
| $\lambda$       |            | Transmittance of the haze layer                       |
| $\alpha_{cano}$ |            | Albedo at the canopy                                  |
| $\alpha_{obs}$  |            | Albedo at the observation height                      |
| $x_L$           | m          | Distance between observation height and canopy height |
| $b_{ext}$       |            | Extinction coefficient                                |
| $x_v$           | m          | Visibility distance                                   |

737 Table 3

738 Comparison of albedo from forest and peatland sites.

739

---

| Site type             | Albedo      | Reference             |
|-----------------------|-------------|-----------------------|
| Tropical peatland     | 0.092–0.099 | This study            |
| Amazonia forest       | 0.114–0.115 | Cescatti et al., 2012 |
| Amazonia forest       | 0.12        | Oliveira et al., 2019 |
| Finnish peat bog      | 0.132       | Gao et al., 2014      |
| Open mesotrophic fen  | 0.137       | Lohila et al., 2010   |
| Open Finnish peatland | 0.140       | Kuusinen et al., 2013 |

---

740

741

742 Appendix

743

744 Monthly albedo (mean  $\pm$  1 standard deviation)

|     | UF                  | DF                  | DB                  |
|-----|---------------------|---------------------|---------------------|
| Jan | 0.0968 $\pm$ 0.0030 | 0.0944 $\pm$ 0.0046 | 0.1000 $\pm$ 0.0166 |
| Feb | 0.0950 $\pm$ 0.0033 | 0.0909 $\pm$ 0.0049 | 0.0973 $\pm$ 0.0185 |
| Mar | 0.0942 $\pm$ 0.0025 | 0.0890 $\pm$ 0.0043 | 0.0940 $\pm$ 0.0174 |
| Apr | 0.0927 $\pm$ 0.0024 | 0.0863 $\pm$ 0.0057 | 0.0873 $\pm$ 0.0208 |
| May | 0.0922 $\pm$ 0.0034 | 0.0874 $\pm$ 0.0063 | 0.0929 $\pm$ 0.0185 |
| Jun | 0.0944 $\pm$ 0.0038 | 0.0892 $\pm$ 0.0055 | 0.0974 $\pm$ 0.0176 |
| Jul | 0.0951 $\pm$ 0.0044 | 0.0910 $\pm$ 0.0053 | 0.1028 $\pm$ 0.0127 |
| Aug | 0.0953 $\pm$ 0.0034 | 0.0906 $\pm$ 0.0043 | 0.1021 $\pm$ 0.0114 |
| Sep | 0.0961 $\pm$ 0.0032 | 0.0938 $\pm$ 0.0039 | 0.1090 $\pm$ 0.0086 |
| Oct | 0.0947 $\pm$ 0.0055 | 0.0901 $\pm$ 0.0053 | 0.1063 $\pm$ 0.0111 |
| Nov | 0.0944 $\pm$ 0.0060 | 0.0919 $\pm$ 0.0059 | 0.1032 $\pm$ 0.0154 |
| Dec | 0.0962 $\pm$ 0.0049 | 0.0967 $\pm$ 0.0056 | 0.1022 $\pm$ 0.0216 |

745

746